

Article

Cost Functions for Generation Dispatching in Microgrids for Non-Interconnected Zones in Colombia

Cristian Hoyos-Velandia¹, Lina Ramirez-Hurtado¹, Jaime Quintero-Restrepo¹ , Ricardo Moreno-Chuquen^{1,*} 
and Francisco Gonzalez-Longatt² 

¹ Faculty of Engineering, Universidad Autónoma de Occidente, Cali 760030, Colombia; cristian.hoyos@uao.edu.co (C.H.-V.); lhurtado@uao.edu.co (L.R.-H.); jqintero@uao.edu.co (J.Q.-R.)

² Department of Electrical Engineering, Information Technology and Cybernetics, University of South-Eastern Norway, 3918 Porsgrunn, Norway; fglongatt@fglongatt.org

* Correspondence: rmoreno@uao.edu.co

Abstract: Generation dispatching is a challenge in islanded microgrids due to the operational and economic restrictions in isolated zones. Furthermore, the impact of usual operational network changes in topology, load demand, and generation availability may become significant considering the grid size. This research paper presents a detailed multiple cost function modeling methodology of an optimal power flow algorithm applied to a non-interconnected zone in Colombia. The optimal power flow (OPF) formulation includes cost functions related to renewable resources as presented in the isolated zone and a complete model of the charging and discharging of batteries. Additionally, the flexibility of the proposal is tested using three different network topologies with a characteristic daily load curve from the zone. The main contribution of this paper lies in the implementation of an optimal power flow including cost functions of renewable sources for isolated microgrids. A test case for a non-interconnected zone in Colombia is performed for various operation cases.

Keywords: batteries; cost functions; DER; microgrids; renewables; storage



Citation: Hoyos-Velandia, C.; Ramirez-Hurtado, L.; Quintero-Restrepo, J.; Moreno-Chuquen, R.; Gonzalez-Longatt, F. Detailed Cost Functions for Generation Dispatching in Microgrids for Non-Interconnected Zones in Colombia. *Energies* **2022**, *15*, 2418. <https://doi.org/10.3390/en15072418>

Academic Editor: Ali Mehrizi-Sani

Received: 28 January 2022

Accepted: 22 March 2022

Published: 25 March 2022

Publisher's Note: MDPI stays neutral with regard to jurisdictional claims in published maps and institutional affiliations.



Copyright: © 2022 by the authors. Licensee MDPI, Basel, Switzerland. This article is an open access article distributed under the terms and conditions of the Creative Commons Attribution (CC BY) license (<https://creativecommons.org/licenses/by/4.0/>).

1. Introduction

Given the massive integration of distributed energy resources (DERs) into electrical power systems, there are microgrids operating either as connected or in islanded mode [1]. There are critical challenges in the operation of microgrids in islanded mode. The dispatch of generation satisfying technical restrictions in order to guarantee the supply at a minimum cost is a present-day problem [2].

There are different definitions for microgrids; from a broad point of view, they correspond to the integration of DERs, including energy storage systems (ESSs) and controllable loads. The DERs include renewable and non-renewable energy sources such as biodigesters, photovoltaic solar systems, and small hydroelectric plants. It is also well-known that in islanded microgrids the network topology, the capacity, and the load demand may change drastically in short periods of time. Therefore, the generated dispatching should consider suitable models for a wide range of generating units and should be flexible to adapt to different operating conditions [3]. Additionally, the appropriate modeling of cost functions is important to obtain optimal operating conditions that satisfy demand requirements. Usually, depending on sites technologies, the cost functions vary.

The research on microgrids covers challenges at the operational level. In particular, the dispatching of renewable sources with storage requires detailed modeling in order to ensure economic conditions under operational restrictions. Furthermore, challenges vary if the microgrid is either islanded or connected to the grid. In islanded microgrids, the management and operation of resources is a critical issue given the generation backup provided in situ. Presently, batteries provide an appropriate asset to deal with the intermittency of primary renewable resources such as solar radiation and wind. Usually, the modeling of

battery energy storage systems has been addressed in the literature considering the state of charge (SoC).

The generation dispatching has been addressed in several papers with emphasis in algorithms for optimal dispatching [4–6]. Some of them have proposed cost functions in order to incorporate particularities of renewable sources. For instance, the modeling of power generation cost functions in real-time operation with renewable sources have been addressed in [7], including fluctuating load. The optimal operation of microgrids with multiple renewable energy sources to achieve minimum operating costs have been performed in [8] for a case with six generating units with an installed capacity of 737 kW, and in the case of [9], including electricity tariffs. There are novelties including unit commitment with ideal and generic energy storage units in order to incorporate the intermittency of renewable resources in [10]. Furthermore, in [4,11] the authors proposes strategies for online management of microgrid with storage considering an economic dispatch. Some authors [12] have implemented voltage-dependent load models. Therefore, these papers use cost functions that correspond to standard cost functions without particularities to each renewable source.

A economic dispatch methodology has been addressed to consider external power exchange over a 24 h period in [5,6], both publications includes microgrids connected to the local network. Recently, optimization methods have been included in order to solve a nonlinear formulation, a second-order cone optimization is proposed in [13] while in [14] mixed-integer linear programming is proposed. Given the interest in optimization solvers, the authors in [15] have implemented a comparative study with various solvers to implement an economic dispatch in two-stages. More recently a bi-level optimal strategy has been addressed in [16] using a consensus algorithm. Iterated algorithms for economic dispatch in a microgrid is proposed in [17]. An economic dispatch approach with bus voltage control for droop-controlled DC microgrids in [18] incorporating control issues in the dispatching.

The main contribution of this paper is the optimal generation dispatching of microgrids operating in non-interconnected zones including detailed cost functions. An optimal power flow is fully implemented to obtain economic dispatch with multiple renewable sources and storage system. A test case for a non-interconnected zone in Colombia is developed to evaluate their performance. The flexibility of the proposed method is tested with different network topologies, load demand and generation availability and considering different operational scenarios. Moreover, in this paper, modeling of storage with batteries is included to obtain accurate results. The full development of the model has been implemented and coded to solve the optimal power flow. The implemented model is tested with different network topologies, load demand and generation availability to analyse different operational scenarios.

This paper contains two additional sections. In Section 2, the notation is presented and the detailed formulation for the optimal power flow considering multiple renewable sources and storage. In Section 3, the results are discussed for different operational conditions including changes in network topology and demand.

2. Formulation for a DC-Based Optimal Power Flow with Renewable Energy Sources (RES)

This section includes the notation and the mathematical formulation for the DC-Based OPF model. This model considers thermal, biomass, solar, wind, and hydro power generation with storage. First, the full notation is presented indicating the nomenclature used. Then, the objective function is presented based on cost minimization, followed by generation restrictions and the corresponding technical limits of charging and discharging of batteries.

2.1. Notation

The nomenclature used in this paper is displayed in this section:

n	Index of the node.
i	Index of generation units.
i, j	Index of network buses connected by transmission branches.
η_c	Charging efficiency of the Energy Storage System.
η_d	Discharging efficiency of the Energy Storage System.
s	Index of storage units.
t	Index of time periods (hours).
l	Index of network branches.
L	Number of network branches.
S	Number of storage units.
T	Time period in the operating horizon, in this case 24 h.
GD	Thermal generation unit.
BM	Biomass generation unit.
MT	Hydro generation unit.
WT	Wind generation unit.
PV	Solar generation unit.
$\rho_{mixture}$	Density of the mixture
C_i	Generation cost from each unit i ([\$/kW])
a_{GD}, b_{GD}, c_{GD}	fuel cost coefficients of the thermal unit GD.
a_{BM}, b_{BM}, c_{BM}	cost coefficients of the biomass unit GD.
$P_{i,t}^{g,max}, P_{i,t}^{g,min}$	Maximum/Minimum limits of power generation unit i in period t (kW).
C_p	Solar and wind stranded cost associated by not generating at their maximum capacity.
$PL_{i,j}^{max}$	Maximum power flow limits of branch connecting bus i to j .
$P_{s,t}^{ch,max}, P_{s,t}^{ch,min}$	Maximum/Minimum of power charged from ESS unit s (kW).
$P_{s,t}^{dch,max}, P_{s,t}^{dch,min}$	Maximum/Minimum of power discharged from ESS unit s (kW).
ESS_s^{max}, ESS_s^{min}	Maximum/Minimum energy stored (kWh) in storage s .
$\theta_{i,t}$	Voltage angle of bus i at time t (rad).
V_n^{max}, V_n^{min}	Maximum/Minimum voltage of node n (p.u).
$P_{i,t}^{ch}, P_{i,t}^{dch}$	Power Charged/discharged to/from ESS connected to bus i at time t (kW).
$D_{i,t}$	Electric power load in bus i at time t .
$DT_{i,t}$	Electric power total load at time t .
$P_{i,t}$	Power generated by unit i at time t (kW).
$PL_{i,t}$	Power flow of branch connecting bus i to j at time t (kW).
P_i^{dch}	Power discharged from ESS unit i at time t (kWh).
P_i^{ch}	Power charged from ESS unit i at time t (kWh).
Av_t^{WT}	Availability of wind turbine connected to bus i at time t (kW).
Av_t^{PV}	Availability of solar system connected to bus i at time t (kW).
P_{nom}^{PV}	Maximum nominal power of wind system.
P_{nom}^{WT}	Maximum nominal power of solar system.
F_c	Fuel consumption.
S_{fc}	Specific fuel consumption.

2.2. Mathematical Formulation

The mathematical formulation of the DC-Based OPF model with RES is discussed in this section. The main aim is to find a minimum total operating cost associated with

generating energy of each source and the energy storage system for a meet load during an interval of time T , this objective function can be described by Equation (1).

$$F_{obj} = \min \sum_{i=1}^n C_i^{GD}[t] + C_i^{BM}[t] + C_i^{MT}[t] + C_i^{WT}[t] + C_i^{PV}[t] + C_i^{ESS}[t] \quad (1)$$

2.2.1. Diesel Generation

According to [7], the cost of conventional fossil fuel generation can be represented as a quadratic function as shown in Equation (2).

$$C_i^{GD}[t] = a_{GD} \cdot P_i^{GD^2}[t] + b_{GD} \cdot P_i^{GD}[t] + c_{GD} \quad (2)$$

where P_{GD} is the power generated from the fossil fuel power plant. From [7,8], a_{GD} is the cost of installing a kW in a generating unit [$\frac{\$}{\text{kWh}^2}$], b_{GD} it is the price of generating one kW in one hour [$\frac{\$}{\text{kWh}}$] and c_{GD} [$\frac{\$}{\text{h}}$] the cost of maintenance. The values a_{GD} , b_{GD} , c_{GD} , are obtained from the relation between fuel consumption vs. power output of a diesel engine given in [8] and adjusted to a value of 8 kW diesel generator. Figure 1 shows a second-order polynomial function obtained to model the behavior of the generation cost. The Equations (3)–(5) show the cost functions. The M value in Equation (3) is related to the efficiency of the engine.

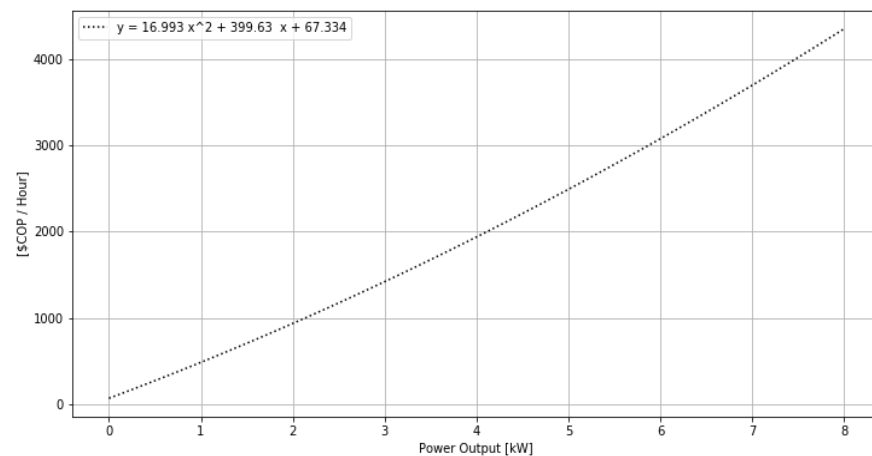


Figure 1. Costs vs. power output of a 8 kW diesel engine.

$$C_i^{GD} = M \cdot P_i^{GD}[t] \quad (3)$$

$$0 \leq P_i^{GD}[t] \leq P^{GD,max} \quad (4)$$

$$C_{GD} = 16.933 \cdot P_i^{GD^2}[t] + 399.63 \cdot P_i^{GD}[t] + 67.734 \quad (5)$$

In Figure 1, the y-axis value is established according to the region of operation. In this work, a region near La Plata, Buenaventura, Colombia, was chosen since it is a non-interconnected area. According to the fuel and lubricant transport costs published by the CREG (Energy and Gas Regulatory Commission) [19], the shipping cost per gallon of diesel fuel from Buenaventura to the Region of La Plata is $740 \left[\frac{\text{COP}}{\text{Gallon}} \right]$. This cost must be added to the discriminated costs of fuel, as shown in the methodology presented in the UPME (Energy and Mining Planning Unit) [20] by. Therefore, the price per gallon obtained was $9615 \left[\frac{\text{COP}}{\text{Gallon}} \right]$.

2.2.2. Biomass Generation

To determine the biomass consumption curve with respect to the generated power some references are reviewed [21–25]. In [23], a test of a machine with a nominal power 3.7 kW and speed of 3000 rpm at five different loads of electrical power are presented. With the information provided, the specific fuel consumption curves are obtained with respect to the power generated by the engine and then the cost (\$ COP/h) is established according to CREG in [26]. In Figure 2, a second-order polynomial cost model is presented for the biomass engine according to the power generated. The cost model considering the power limits of the diesel generator is shown in Equation (6), where a_{BM} is replaced by the quantification of specific fuel consumption (S_{fc}) in Equation (7). Equation (8) represents the technical constraints of the unit, and finally, the values are shown in Equation (9).

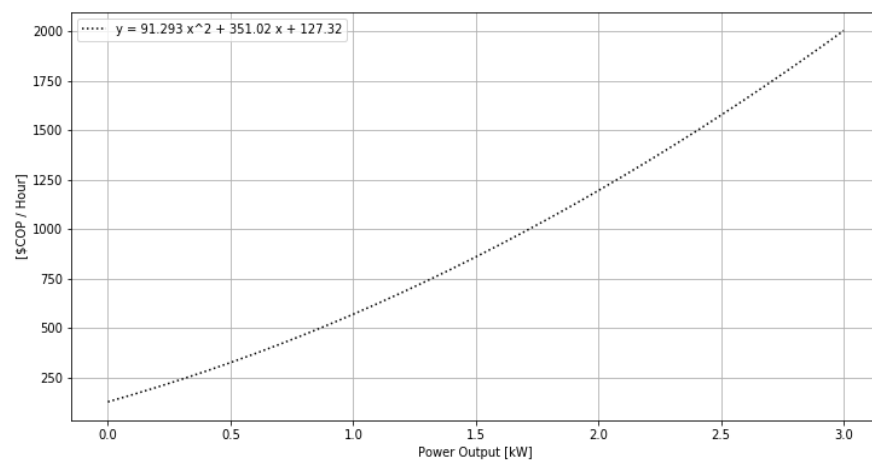


Figure 2. Costs vs. power output of a 3 kW biomass engine.

$$C_i^{BM}[t] = a_{BM} * P_i^{BM^2}[t] + b_{BM} * P_i^{BM}[t] + c_{BM} \quad (6)$$

$$a^{BM}[t] = S_{fc} = \frac{F_C * \rho_{mixture}}{P_{BM}^{max} * t} \quad (7)$$

$$0 \leq P_i^{BM}[t] \leq P^{BM,max} \quad (8)$$

$$C_i^{BM}[t] = 91.293 * P_i^{BM^2}[t] + 351.02 * P_i^{BM}[t] + 127.32 \quad (9)$$

2.2.3. Microturbine Generation

Equation (10) indicates the power generation by the hydro source. Only the costs associated with operation and maintenance (O&M) are established as a cost function [27–29], and a penalty cost C_p , for not making the maximum use of the available resource.

$$C_i^{MT}[t] = (P_i^{MT, max} - P_i^{MT}[t]) \cdot C_p + C_{inv} \quad (10)$$

C_{inv} is a function of the annual investment cost, representing the (O&M) costs. Annual operating and maintenance costs are normally quoted as a percentage of the investment cost per year. Typical values vary between 1% and 4%, depending on the capacity of the hydroelectric plant [30]. In this case, the hydraulic generation for the considered region is 3 kW, the value of the investment cost of 52 $\left[\frac{US}{kW}\right]$ year is obtained for this project and in terms of Colombian pesos per kWh is shown in Equation (11).

$$C_{inv} = 52 \frac{US\$}{kW \cdot year} \cdot \frac{1 \text{ year}}{365 \text{ days}} \cdot \frac{1 \text{ day}}{24 \text{ h}} \cdot \frac{CO\$ 3553}{1 \text{ US\$}} = 21.09 \text{ CO\$/kWh} \quad (11)$$

2.2.4. Solar and Wind Generation

The cost of solar and wind energy should be assumed to be the minimum possible value and be dispatched at the maximum power that they can generate as shown by Equations (13) and (15). Both solar and wind energy are formulated with the same equations as expressed in Equations (12) and (14).

$$C_i^{WT}[t] = (P_i^{WT,Max}[t] - P_i^{WT}[t]) * C_n + C_{WT} * P_i^{WT}[t] \quad (12)$$

$$P_i^{WT,Max}[t] = Av_{i,t}^{WT} * P_{nom}^{WT} \quad (13)$$

$$C_i^{PV}[t] = (Av_{i,t}^{PV}[t] - P_i^{PV}[t]) * C_n + C_{PV} * P_i^{PV}[t] \quad (14)$$

$$P_i^{PV,Max}[t] = Av_{i,t}^{PV}[t] * P_{nom}^{PV} \quad (15)$$

2.2.5. Battery Energy Storage System (ESS) Model

Finally, Equation (16) expresses the model for an ESS model where the variables may not charge and discharge simultaneously [31,32]. The ESS proposed to have some constraints as the technical limits of charging, discharging and storage as shown in Equations (17)–(19).

$$ESS[t] = ESS[t - 1] + \eta_{ch} * P_{s,t}^{dch} - \frac{1}{\eta_{dch}} * P_{s,t}^{dch} \quad (16)$$

$$P_{s,t}^{dch,min} \leq P_{s,t}^{dch} \leq P_{s,t}^{dch,max} \quad (17)$$

$$P_{s,t}^{ch,min} \leq P_{s,t}^{ch} \leq P_{s,t}^{ch,max} \quad (18)$$

$$ESS_s^{min} \leq ESS_s \leq ESS_s^{max} \quad (19)$$

The OPF model proposed in Equation (1), considers various restrictions that make the DC power flow feasible as: first, voltage magnitudes are approximately 1.00 p.u. and the angle of the slack bus is assumed to be zero as the reference for the rest of the grid [33] as presented in Equations (20) and (21). The power flowing on each line is specified by Equation (22). The power balance is given by Equation (23). The technical unit limits are given by Equation (24). As well, power flow on each line is expressed in Equation (25). Finally, angle and voltage limits on each node are shown in Equations (26) and (27).

$$v_i \approx v_j \approx 1 \quad (20)$$

$$\theta_{slack,t} = 0 \quad (21)$$

$$P_{i,j} = \frac{\theta_{i,t} - \theta_{j,t}}{x_{i,j}} \quad (22)$$

$$\sum P_{i,t} - \sum D_{i,t} + \sum (P_{s,t}^{ch} - P_{s,t}^{dch}) = \sum PL_{i,t} \quad (23)$$

$$P_{i,t}^{min} \leq P_{i,t} \leq P_{i,t}^{max} \quad (24)$$

$$-PL_{i,j}^{min} \leq PL_{i,j} \leq PL_{i,j}^{max} \quad (25)$$

$$\frac{-\pi}{2} \leq \theta_{n,t} \leq \frac{\pi}{2} \quad (26)$$

$$V_n^{min} \leq V_n \leq V_n^{max} \quad (27)$$

3. Results and Discussion

This section shows the results of three network topologies that were studied and analyzed. The performance is evaluated for a 24-h period. All simulations were completed

by a personal computer (PC) running Windows® with an Intel® Core I5+8300H processor @1.6 GHz with 16.00 GB RAM, using Gurobi® Solver (9.1.2) [34] under the JuMP 0.20.1 Julia platform [35]. Gurobi is a commercial solver for optimization problems with the flexibility to be implemented.

The implemented optimal power flow for generating dispatching of microgrids has the following main features: flexibility and scalability, by allowing testing different demand power profiles, different solar and wind profiles, as well as various network topologies. The selected region was a non-interconnected zone in the pacific zone of Colombia known as La Plata, Bahia Malaga in Colombia. The solar and wind profiles are described below.

3.1. Simulation

3.1.1. Solar and Wind Scenario

The RES and ESS performance were evaluated considering climate data of the zone provided by [36,37]. The resource availability in the region of La Plata, Bahia Malaga can be seen in Figure 3.

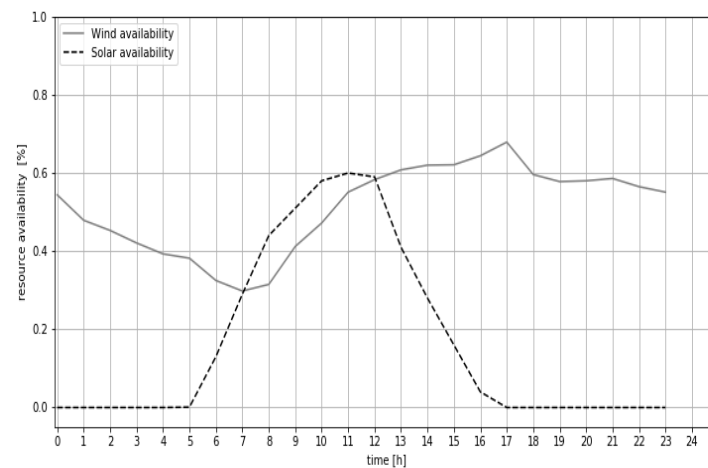


Figure 3. Normalized resource availability in the region of La Plata, Bahía Málaga.

3.1.2. Load Curve Description

The load curves are seen in Figure 4 with profiles for various load factors.

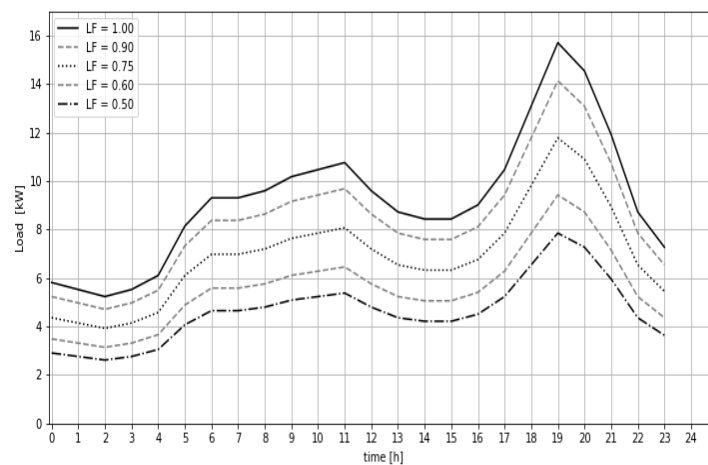


Figure 4. Daily Load curves profiles for the system.

3.1.3. Topologies

Three network topologies are used to test the proposed generating dispatch approach in non-interconnected zones. Usually, microgrids operate in topologies known as a single bus, radial, and tree for isolated microgrids [38]. Given the cases studied in this paper, tree topology is used, it represents typical configurations given the low demand level with few customers in the isolated areas of Colombia. The topological graph looks like a tree with different branches either supplying electricity to loads or connected to distributed energy sources. This section shows the single-line diagrams, reactance values, line boundaries and the location of resources.

Topology 1 is a radial five-bus network in which five generators (wind, biomass, solar, hydro and thermal), a storage system with batteries and four loads are connected, as shown in the one-line diagram in Figure 5. Their technical characteristics can be consulted in Table 1.

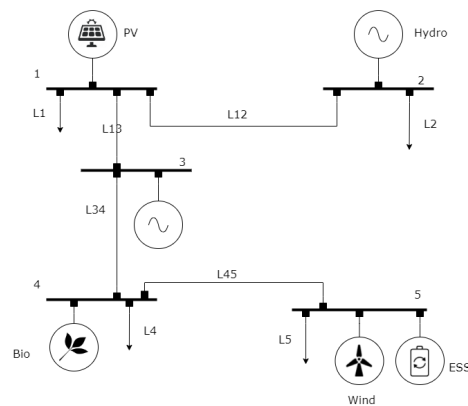


Figure 5. One-line diagram: Topology 1. 5-bus power system.

Radial topology 2 correspond to the IEEE 37-node California distribution system [39]. It is a 5-bus network in which five generators, an ESS and four loads are connected, as shown in the one-line diagram in Figure 6. This description can be seen in Table 2.

Table 1. Topology 1. 5-bus power system data.

Gen	Bus	P_g^{min} (kW)	P_g^{max} (kW)	Line	Reactance (Ω)	Limits Lines (kW)
1	1	0	3	L_{12}	0.051	$-18.8 \leq PL_{12} \leq 18.8$
2	2	0	3	L_{13}	0.064	$-18.8 \leq PL_{13} \leq 18.8$
3	3	0	8	L_{34}	0.064	$-18.8 \leq PL_{34} \leq 18.8$
4	4	0	3	L_{45}	0.050	$-18.8 \leq PL_{45} \leq 18.8$
5	5	0	3	-	-	-

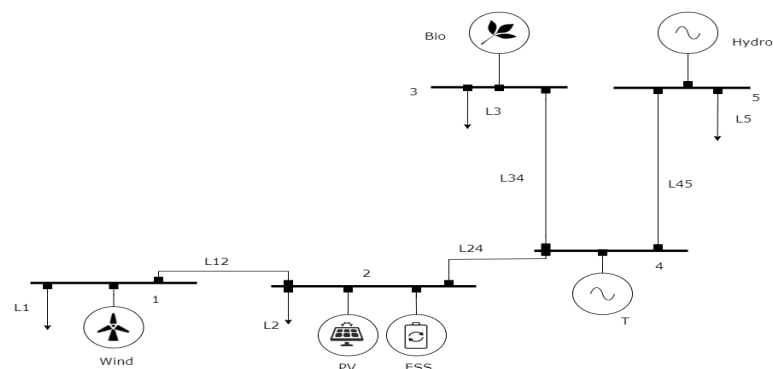


Figure 6. One-line diagram: topology 2. 5-bus power system.

Table 2. Topology 2. 5-bus power system data.

Gen	Bus	P_g^{min} (kW)	P_g^{max} (kW)	Line	Reactance (Ω)	Limits Lines (kW)
1	2	0	3	L_{12}	0.111	$-18.8 \leq PL_{12} \leq 18.8$
2	5	0	3	L_{24}	0.132	$-18.8 \leq PL_{13} \leq 18.8$
3	4	0	8	L_{34}	0.014	$-18.8 \leq PL_{34} \leq 18.8$
4	3	0	3	L_{45}	0.018	$-18.8 \leq PL_{45} \leq 18.8$
5	1	0	3	-	-	-

Finally, topology 3 has as its main features solar and wind systems in the same bus, as shown in Figure 7. The parameters are listed in Table 3.

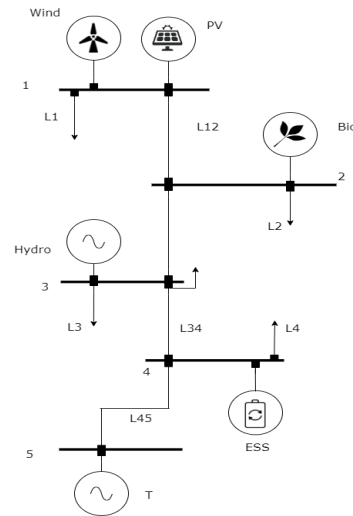


Figure 7. One-line diagram: topology 3. 5-bus power system.

Table 3. Third topology 5-bus power system data.

Gen	Bus	P_g^{min} (kW)	P_g^{max} (kW)	Line	Reactance (Ω)	Limits Lines (kW)
1	1	0	3	L_{12}	0.056	$-18.8 \leq PL_{12} \leq 18.8$
2	3	0	3	L_{23}	0.120	$-18.8 \leq PL_{13} \leq 18.8$
3	5	0	8	L_{34}	0.032	$-18.8 \leq PL_{34} \leq 18.8$
4	2	0	3	L_{45}	0.005	$-18.8 \leq PL_{45} \leq 18.8$
5	1	0	3	-	-	-

For all topologies presented, the cost of generators is seen in Table 4. The results and the corresponding analysis are developed in the next sections.

Table 4. Generation cost of each unit.

Generator	Resource	Function Cost
1	PV	$C_i^{PV}[t] = (Av_{i,t}^{PV} - P_i^{PV}[t]) * 399.73 + P_i^{PV}[t]$
2	Hyd	$C_i^{MT}[t] = (P_i^{MT,Max} - P_i^{MT}[t]) + 21.09$
3	T	$C_i^{GD}[t] = 16.933 * P_i^{GD^2}[t] + 399.63 * P_i^{GD}[t] + 67.734$
4	Bio	$C_i^{BM}[t] = 91.293 * P_i^{BM^2}[t] + 351.02 * P_i^{BM}[t] + 127.32$
5	Wind	$C_i^{WT}[t] = (Av_{i,t}^{WT} - P_i^{WT}[t]) * 399.73 + P_i^{WT}[t]$

3.2. Analysis of Topologies

This section shows the analysis of the proposed methodology applied to each case at $LF = 0.60$ seen in Figure 3. For all scenarios, the battery on the energy storage takes

advantage of times when the availability of power from renewable sources exceeds the demand values and charge the system. Figure 8 shows the optimal power flow results for the topology 1.

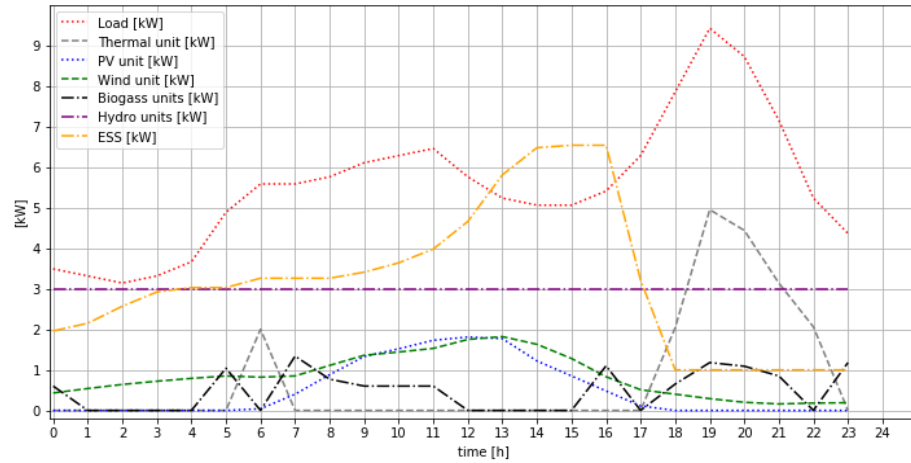


Figure 8. Performance by each unit in topology 1 at load factor to 60%.

The microgrid’s performance using renewable energies to maximum values can be observed in hours 0, 9, 10 and 11 when the battery is charged with the surplus power available from renewable energies. However, for this, biogas is used in its technical minimum to cover the energy demand in its bus, and at hour 6, the battery is charged but with the use of the thermal unit in its technical minimum.

The battery energy storage system is charged in hours 1, 2, 3, 4, 12, 13, 14 and 15, but use the surplus power available from renewable sources to cover the demand. In Table 5, the behavior of the power generated by each of the sources and the battery for each hour are shown.

Table 5. Topology 3. 5-bus power system data.

Hour	Load	P_{GD} (kW)	P_{PV} (kW)	P_{WT} (kW)	P_{BM} (kW)	P_{MT} (kW)	S_oC (kW)
0	3.49	0.00	0.00	0.43	0.60	3.00	1.96
1	3.31	0.00	0.00	0.54	0.00	3.00	2.15
2	3.15	0.00	0.00	0.64	0.00	3.00	2.57
3	3.31	0.00	0.00	0.72	0.00	3.00	2.92
4	3.66	0.00	0.00	0.79	0.00	3.00	3.03
5	4.90	0.00	0.00	0.85	1.04	3.00	3.03
6	5.58	2.00	0.04	0.82	0.00	3.00	3.26
7	5.58	0.00	0.40	0.85	1.34	3.00	3.26
8	5.76	0.00	0.88	1.11	0.77	3.00	3.26
9	6.11	0.00	1.33	1.36	0.60	3.00	3.41
10	6.28	0.00	1.52	1.44	0.60	3.00	3.64
11	6.46	0.00	1.73	1.53	0.60	3.00	3.98
12	5.76	0.00	1.81	1.75	0.00	3.00	4.66
13	5.24	0.00	1.77	1.82	0.00	3.00	5.81
14	5.06	0.00	1.22	1.63	0.00	3.00	6.48
15	5.06	0.00	0.85	1.28	0.00	3.00	6.54
16	5.41	0.00	0.48	0.83	1.10	3.00	6.54
17	6.29	0.00	0.11	0.51	0.00	3.00	3.21
18	7.86	2.04	0.00	0.40	0.65	3.00	1.00
19	9.43	4.95	0.00	0.29	1.18	3.00	1.00
20	8.73	4.44	0.00	0.20	1.09	3.00	1.00
21	7.16	3.14	0.00	0.16	0.85	3.00	1.00
22	5.24	2.06	0.00	0.18	0.00	3.00	1.00
23	4.36	0.00	0.00	0.19	1.18	3.00	1.00

The battery energy storage system is discharged in hour 17, while in hour 18, the battery is discharged to the minimum allowed value (1 kWh), and the rest of the demand is covered by the thermal and biomass generator

In the other hours where there is no charging/discharging of the batteries, the renewable energy generation units are used to its maximum power production, and any surplus generation is stored in the batteries energy storage system, maintaining more active participation of the batteries in the optimal power flow.

The results for topologies 2 and 3 are given in Figure 3. Similar analysis results are shared in topology 1 in Figure 8. The primary differences concerning the topology 1 are in power flows, the generations sources in load buses have been dispatched at specific values to avoid transmission losses. The results obtained for topology 2 can be seen in Figure 9 and for topology 3, in Figure 10.

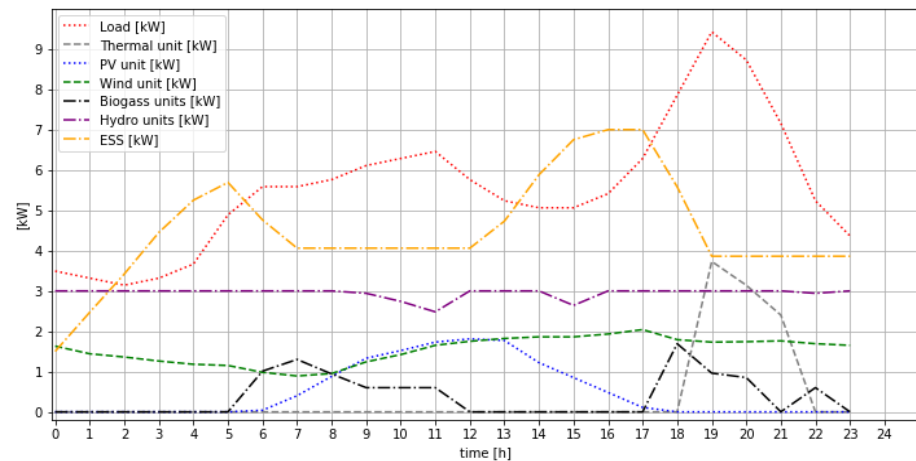


Figure 9. Performance by each unit in topology 2 at load factor to 60%.

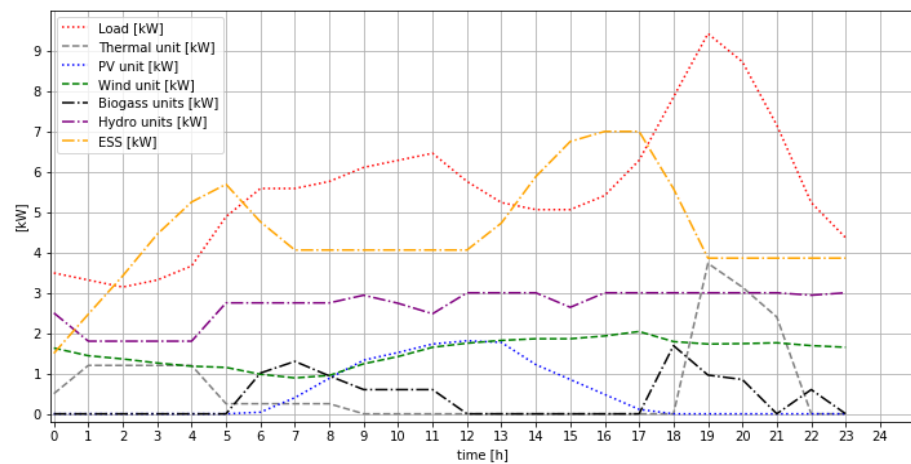


Figure 10. Performance by each unit in topology 3 at load factor to 60%.

Figure 10 shows that in topology 3, the use of the thermal unit is favored over the hydro unit, because the cost of transmission through the lines from bus 1, 2 and 3 is higher than that presented in 5. However, this is only reflected in the first hours. Once the solar system starts operating, the thermal unit is attenuated, taking advantage of the energy on-site of the RES. The ESS, similar to the first model, is charged when the renewable units are available and once they cannot operate at its maximum capacity due to environmental conditions; it delivers its energy, reducing operating costs.

The conditions proposed in this formulation, the topology with the minimum objective value is the topology two, where the closest connection of the ESS to solar and wind renewable energies allow the reduction of the system costs. Finally, Table 6 compares the objective values of topologies together with the traditional network.

Table 6. Comparison of cost of energy for systems and traditional grid network.

Topology	Objective Value \$[COP]	Price of kWh \$[COP]
1	\$25.240	\$189
2	\$24.278	\$182
3	\$26.143	\$196
Traditional Grid Network	\$69.000	\$518

4. Conclusions

The proposed formulation for generation dispatching of microgrids in non-interconnected zones is tested different demand profiles and different profiles of solar and wind generation depending on the time of year and the geographical location of the region where the microgrid is implemented. It was possible to observe the operation for the charging and discharging of the battery during the tests at different demand values. The fulfillment of the power balance and the balance of the flow were demonstrated through the distribution system according to its capacities.

In particular, the implemented optimal power is flexible because it allows changes in the network topology such as number of nodes, number of lines, and cost functions, among others parameters. Finally, the results of this research reveal that the economic operation of microgrids with multiple renewable sources and storage systems in non-interconnected zones is a challenge of interest for applied research. The economic dispatch of generation could increase the feasibility of microgrids project in isolated zones given that the resources are used at optimum levels of dispatching.

Author Contributions: Conceptualisation, J.Q.-R.; methodology, L.R.-H. and C.H.-V.; software, C.H.-V. and L.R.-H.; validation, F.G.-L. and R.M.-C.; formal analysis, J.Q.-R. and F.G.-L.; investigation, L.R.-H.; resources, J.Q.-R.; data curation, C.H.-V.; writing—original draft preparation, C.H.-V. and L.R.-H.; writing—review and editing, F.G.-L. and R.M.-C.; visualisation, F.G.-L.; supervision, J.Q.-R. and R.M.-C.; project administration, J.Q.-R. All authors have read and agreed to the published version of the manuscript.

Funding: This research received no external funding.

Institutional Review Board Statement: Not applicable.

Informed Consent Statement: Not applicable.

Data Availability Statement: The data that support the tool development are available from the corresponding author, by prior request.

Acknowledgments: The authors would like to thank the support of the Universidad Autónoma de Occidente in Cali, Colombia.

Conflicts of Interest: The authors declare no conflict of interest.

Abbreviations

The following abbreviations are used in this manuscript:

ESS	Energy storage system
OPF	Optimal power flow
RES	Renewable energy source
DC	Direct current

References

- Hirsch, A.; Parag, Y.; Guerrero, J. Microgrids: A review of technologies, key drivers, and outstanding issues. *Renew. Sustain. Energy Rev.* **2018**, *90*, 402–411. [[CrossRef](#)]
- Stadler, M.; Naslé, A. Planning and implementation of bankable microgrids. *Electr. J.* **2019**, *32*, 24–29. [[CrossRef](#)]
- Jung, J.; Villaran, M. Optimal planning and design of hybrid renewable energy systems for microgrids. *Renew. Sustain. Energy Rev.* **2017**, *75*, 180–191. [[CrossRef](#)]

4. Xiaoping, L.; Ming, D.; Jianghong, H.; Pingping, H.; Yali, P. Dynamic economic dispatch for microgrids including battery energy storage. In Proceedings of the 2nd International Symposium on Power Electronics for Distributed Generation Systems, Hefei, China, 16–18 June 2010; pp. 914–917.
5. Zachar, M.; Daoutidis, P. Economic dispatch for microgrids with constrained external power exchange. *IFAC-PapersOnLine* **2016**, *49*, 833–838. [[CrossRef](#)]
6. Balducci, P.; Mongird, K.; Wu, D.; Wang, D.; Fotedar, V.; Dahowski, R. An evaluation of the economic and resilience benefits of a microgrid in Northampton, Massachusetts. *Energies* **2020**, *13*, 4802. [[CrossRef](#)]
7. El-Faouri, F.S.; Alzahlan, M.W.; Batarseh, M.G.; Mohammad, A.; Za'ter, M.E. Modeling of a microgrid's power generation cost function in real-time operation for a highly fluctuating load. *Simul. Model. Pract. Theory* **2019**, *94*, 118–133. [[CrossRef](#)]
8. Duláu, L.I.; Bicá, D. Optimization of generation cost in a microgrid. *Procedia Manuf.* **2018**, *22*, 703–708. [[CrossRef](#)]
9. Jamaica-Obregón, J.; Moreno-Chuquen, R.; Flórez-Cediel, O. Optimal Operation of Grid-Connected Microgrids with Photovoltaic Generation and Storage. *Int. Rev. Electr. Eng. (IREE)* **2021**, *16*, 50. [[CrossRef](#)]
10. Pozo, D.; Contreras, J.; Sauma, E.E. Unit commitment with ideal and generic energy storage units. *IEEE Trans. Power Syst.* **2014**, *29*, 2974–2984. [[CrossRef](#)]
11. Mohamed, F.A.; Koivo, H.N. System modelling and online optimal management of microgrid with battery storage. In Proceedings of the 6th International Conference on Renewable Energies and Power Quality (ICREPO'07), Sevilla, Spain, 28–30 March 2007; pp. 26–28.
12. Montoya, O.D.; Gil-González, W.; Grisales-Noreña, L.; Orozco-Henao, C.; Serra, F. Economic dispatch of BESS and renewable generators in DC microgrids using voltage-dependent load models. *Energies* **2019**, *12*, 4494. [[CrossRef](#)]
13. Gil-González, W.; Montoya, O.D.; Grisales-Noreña, L.F.; Cruz-Peragón, F.; Alcalá, G. Economic Dispatch of Renewable Generators and BESS in DC Microgrids Using Second-Order Cone Optimization. *Energies* **2020**, *13*, 1703. [[CrossRef](#)]
14. Sigalo, M.B.; Pillai, A.C.; Das, S.; Abusara, M. An Energy Management System for the Control of Battery Storage in a Grid-Connected Microgrid Using Mixed Integer Linear Programming. *Energies* **2021**, *14*, 6212. [[CrossRef](#)]
15. Lee, G.H.; Park, J.Y.; Ham, S.J.; Kim, Y.J. Comparative study on optimization solvers for implementation of a two-stage economic dispatch strategy in a microgrid energy management System. *Energies* **2020**, *13*, 1096. [[CrossRef](#)]
16. Lyu, Z.; Yang, X.; Zhang, Y.; Zhao, J. Bi-level optimal strategy of islanded multi-microgrid systems based on optimal power flow and consensus Algorithm. *Energies* **2020**, *13*, 1537. [[CrossRef](#)]
17. Modiri-Delshad, M.; Koochi-Kamali, S.; Taslimi, E.; Kaboli, S.H.A.; Rahim, N.A. Economic dispatch in a microgrid through an iterated-based algorithm. In Proceedings of the 2013 IEEE Conference on Clean Energy and Technology (CEAT), Langkawi, Malaysia, 18–20 November 2013. [[CrossRef](#)]
18. Cheng, Z.; Li, Z.; Liang, J.; Gao, J.; Si, J.; Li, S. Distributed economic power dispatch and bus voltage control for droop-controlled DC microgrids. *Energies* **2019**, *12*, 1400. [[CrossRef](#)]
19. Comisión de Regulación de Energía y Gas (CREG), Circular 069-2017. Matriz de costos de transporte de combustible y lubricante, 2017. Available online: <http://apolo.creg.gov.co> (accessed on 3 March 2021).
20. Unidad de Planeación Minero Energética UPME. *Proyección de Precios de los Energéticos Para Generación Eléctrica 2016–2035*; Unidad de Planeación Minero Energética UPME: Bogotá, Colombia, 2016.
21. Rojas-González, A.; Chaparro-Anaya, Ó.; Ospina, C.A. Assessment of biodiesel-diesel blends for producing electric energy. *Ing. Univ.* **2011**, *15*, 319–336.
22. Guerrero, F.O.C.; Maraví, J.L.C. *Generación de Energía Eléctrica con un Motor de Combustión Interna Usando Biodiesel de Aceite de piñón (*Jatropha curcas*)*; Anales Científicos; Universidad Nacional Agraria La Molina: Lima, Peru, 2016; Volume 77, pp. 338–345.
23. Calligiuri, C.; Renzi, M.; Bietresato, M.; Baratieri, M. Experimental investigation on the effects of bioethanol addition in diesel-biodiesel blends on emissions and performances of a micro-cogeneration system. *Energy Convers. Manag.* **2019**, *185*, 55–65. [[CrossRef](#)]
24. Elkelay, M.; Bastawissi, H.A.E.; Esmail, K.K.; Radwan, A.M.; Panchal, H.; Sadasivuni, K.K.; Ponnamma, D.; Walvekar, R. Experimental studies on the biodiesel production parameters optimization of sunflower and soybean oil mixture and DI engine combustion, performance, and emission analysis fueled with diesel/biodiesel blends. *Fuel* **2019**, *255*, 115791. [[CrossRef](#)]
25. Seraç, M.R.; Aydın, S.; Yılmaz, A.; Şevik, S. Evaluation of comparative combustion, performance, and emission of soybean-based alternative biodiesel fuel blends in a CI engine. *Renew. Energy* **2020**, *148*, 1065–1073. [[CrossRef](#)]
26. Comisión de Regulación de Energía y Gas. *D-089-16 Propuesta de Metodología y Parámetros de Referencia del Ingreso al Productor de Biocombustibles*; Comisión de Regulación de Energía y Gas: Bogotá, Colombia, 2017.
27. Ramabhotla, S.; Bayne, S.; Giesselmann, M. Operation and maintenance cost optimization in the grid connected mode of microgrid. In Proceedings of the 2016 IEEE Green Technologies Conference (GreenTech), Kansas City, MO, USA, 6–8 April 2016; pp. 56–61.
28. Tariq, F.; Alelyani, S.; Abbas, G.; Qahmash, A.; Hussain, M.R. Solving renewables-integrated economic load dispatch problem by variant of metaheuristic bat-inspired algorithm. *Energies* **2020**, *13*, 6225. [[CrossRef](#)]
29. Radosavljević, J.; Jevtić, M.; Klimenta, D. Energy and operation management of a microgrid using particle swarm optimization. *Eng. Optim.* **2016**, *48*, 811–830. [[CrossRef](#)]
30. International Renewable Energy Agency. Hydropower. *IRENA* **2012**, *1*. Available online: https://www.irena.org/-/media/Files/IRENA/Agency/Publication/2012/RE_Technologies_Cost_Analysis-HYDROPOWER.pdf (accessed on 3 March 2022).

31. Castillo, A.; Gayme, D.F. Profit maximizing storage allocation in power grids. In Proceedings of the 52nd IEEE Conference on Decision and Control, Firenze, Italy, 10–13 December 2013; pp. 429–435.
32. Cantillo, S.; Moreno, R. Power system operation considering detailed modelling of energy storage systems. *Int. J. Electr. Comput. Eng.* **2021**, *11*, 182–200. [[CrossRef](#)]
33. Wood, A.; Wollenberg, B. *Power Generation, Operation and Control*, 3rd ed.; Wiley: New York, NY, USA, 2014.
34. Gurobi Optimization LLC. Gurobi Optimizer Reference Manual. 2021. Available online: <https://www.gurobi.com/> (accessed on 10 January 2022).
35. Dunning, I.; Huchette, J.; Lubin, M. JuMP: A modeling language for mathematical optimization. *SIAM Rev.* **2017**, *59*, 295–320. [[CrossRef](#)]
36. Pfenninger, S.; Staffell, I. Long-term patterns of european PV output using 30 years of validated hourly reanalysis and satellite data. *Energy* **2016**, *114*, 1251–1265. [[CrossRef](#)]
37. Staffell, I.; Pfenninger, S. Using bias-corrected reanalysis to simulate current and future wind power output. *Energy* **2016**, *114*, 1224–1239. [[CrossRef](#)]
38. Hatziargyriou, N. *Microgrids: Architectures and Control*; John Wiley & Sons: Hoboken, NJ, USA, 2014.
39. Dimeas, A.L.; Hatziargyriou, N.D. Operation of a multiagent system for microgrid control. *IEEE Trans. Power Syst.* **2005**, *20*, 1447–1455. [[CrossRef](#)]